UC Berkeley
UC Berkeley Previously Published Works

Title

Microsecond and nanosecond polyproline II helix formation in aqueous nanodrops measured by mass spectrometry

Permalink

Journal

ISSN

Authors

Mortensen, Daniel N
Williams, Evan R

Publication Date

DOI

Peer reviewed

Microsecond and Nanosecond Polyproline II Helix Formation in Aqueous Nanodrops Measured by Mass Spectrometry

Daniel N. Mortensen and **Evan R. Williams**[*]

Department of Chemistry, University of California, Berkeley, California 94720-1460, United States.

Abstract

The 1.5 µs and <400 ns time constants for the formation of polyproline II helix structures in 21 and 16 residue peptides, respectively, are measured using rapid mixing from theta-glass emitters coupled with mass spectrometry. Results from these studies should serve as useful benchmarks for comparison with computational simulation results.

Secondary structures in proteins and peptides, such as α-helices and β-sheets, can form within tens of microseconds or less.[1,2] Explicit-solvent, all-atom simulations now enable folding trajectories of α-helix and β-structures in biopolymers containing up to 100 amino acids to be computed.[2,3] However, the formation kinetics of other common secondary protein structures, such as that of the polyproline II (PPII) helix, have not been investigated as thoroughly. The PPII helix is an extended left-handed helix with three residues per turn, 3-fold rotational symmetry, and a per residue length of 3.1 Å.[4,5] PPII helices are the primary component of the triple-helix structure of collagen[6] and are commonly found in both natively folded[7-10] and natively unfolded (or disordered)[8,11,12] proteins and peptides. PPII helix structures can occur in polypeptides containing few or no proline residues [13,14] and have been implicated in numerous functional roles,[4,5] including protein-protein interactions,[9] ligand and non-covalent cofactor binding,[15-17] and even in the formation of the amyloid plaques associated with diseases involving protein misfolding, such as Parkinson's.[5,18,19]

The transitions for several individual peptides between a polyproline I (PPI) helix structure in a mostly organic solution to a PPII helix structure in a mostly aqueous solution have been investigated and occur within minutes to hours, depending on the reaction temperature and on the amino-acid sequence.[20-22] Formation kinetics of PPII helices in more native-like buffered aqueous solutions, however, have not been measured. Recently, double-barrel nano-electrospray ionization (nanoESI) emitters, also known as theta-glass emitters, have been used to rapidly mix solutions during nanoESI to investigate numerous room-temperature reactions,[23-27] including monitoring protein folding reactions that occur in microseconds.[26,27] A 2.2 µs folding time constant for the formation of a β-hairpin in a 14 residue peptide was determined, which is the fastest folding event that has been directly

---

[*]*erw@berkeley.edu.*

measured with a rapid mixing technique.[27] Reaction times of between 1 and 22 μs have been achieved with thes e devices by varying the solution flow rate, which depends on the backing pressure and on the nanoESI-emitter tip size.[27] Here, rapid mixing with theta-glass emitters is used to investigate the rates of formation for PPII helices in two short (16 and 21 re sidue) peptides. These peptides are prepared in acidified aqueous solutions in which they are highly unfolded and mixed with buffered aqueous solutions during nanoESI to increase the solution pH and induce the formation of the PPII helices. These structura l transitions are measured using mass spectrometry, and information about the equilibrium structures of the peptides is obtained with circular dichroism (CD).

Mass spectra are acquired using a 9.4 T Fourier-transform ion cyclotron resonance mass spectrometer that is described elsewhere.[28] Rapid mixing and ion formation are performed using theta glass capillaries (Warner Instruments, LLC; Hamden, CT) pulled into tips with outer diameters of between 1465 ± 134 and 244 ± 61 nm using a model p-87 Flaming/ Brown micropipette puller (Sutter Instruments Co., Novato, CA). Grounded platinum wires are brought into contact with the solutions in the emitters, and a backing pressure of either 5 or 10 psi is applied to the back end of the capillary, depending on the desired reaction time.[27] NanoESI is initiated by applying about a −700 V potential to the heated capillary of the ESI interface. Average charges are computed as abundance weighted sums of the charge states, and uncertainties are standard deviations from triplicate measurements. CD spectra are acquired using a model 410 circular dichroism spectrometer (Aviv Biomedical Inc., Lakewood, NJ).

Solutions of [Asp^{76}]-parathyroid hormone fragment 64–84 (amino-acid sequence: EKSLG EADKA DVDVL TKAKS Q) and neurogranin fragment 28–43 (amino-acid sequence: AAKIQ ASFRG HMARK K) are prepared with 10 μM analyte concentrations. The initial pH of droplets formed during the rapid mixing experiments is estimated to be 4.7 ± 0.3. This value is determined using the initial concentrations of acetic acid ($pK_a = 4.8$) and ammonia ($pK_b = 4.8$, both at 25 °C)[29] in the droplets. Initial concentrations in the nanodrops are determined from the initial concentrations of the solutions in each barrel and the relative flow rates of these solutions during nanoESI. Relative flow rates are determined using Leu- and Met-enkephalin as internal standards as described previously.[25]

CD spectra of parathyroid hormone fragment 64-84 (PTH$_{64-84}$) in both a 100 mM aqueous acetic acid solution (pH = 2.9) and the acetic acid solution mixed with a 100 mM aqueous ammonium acetate solution at a 1:1 ratio (equilibrium, pH = 4.7) are shown in Fig. 1 as dashed red and solid blue lines, respectively. There are negative peaks at   200 and 223 nm in both spectra. These peaks are at similar wavelengths as those in the CD spectrum of the seven residue peptide XAO in a buffered aqueous solution at pH = 7.0, which has negative peaks at 198 and 227 nm.[13] XAO has significant PPII helix structure (50%), as well as some β-structures, including turns.[13,14] The similarities between the CD spectrum reported here for PTH$_{64-84}$ and that reported previously for XAO suggest that PTH$_{64-84}$ is composed primarily of PPII helix structures and likely contains some β-structures. These results are consistent with dark field electron microscopy results reported for intact parathyroid hormone in 80 mM aqueous ammonium acetate nanodrops (pH = 7.4),[30] which indicate that residues 69–82 of parathyroid hormone adopt a helical structure and residues 65–68 adopt a

turn structure. The intensities of the peaks at 200 and 223 nm in Fig. 1 are ~2.8 and ~2.6 times greater, respectively, in the CD spectrum of the mixed solution at equilibrium than in that of the acetic acid solution. This result indicates that the structures corresponding to the peaks at 200 and 223 nm are disrupted to a significant extent in the acetic acid solution.

NanoESI of PTH_{64-84} in the acetic acid solution (pH = 2.9) results in the formation of the 3+ and 4+ charge states with an average charge of 3.70 ± 0.02 (Fig. 2a). NanoESI of the acetic acid solution mixed with the ammonium acetate solution at a 1:1 ratio prior to nanoESI (equilibrium, pH = 4.7) results in the 2+ and 3+ charge states with an average charge of 2.80 ± 0.01 (Fig. 2b). The extent of charging for protein and peptide ions in nanoESI depends on many factors, but solution-phase conformation is one of the most important. Folded conformers charge less than unfolded conformers.[31,32] Therefore, the lower average charge obtained with the mixed solution at equilibrium (2.80) than with the acetic acid solution (3.70) is consistent with PTH_{64-84} adopting a more folded structure in the mixed solution than in the acetic acid solution. The 2+ and 3+ charge states comprise ~3.3 times more of the population with the mixed solution at equilibrium (100%, Fig. 2b) than with the acetic acid solution ($30 \pm 2\%$, Fig. 2a). This result is consistent with the ~2.8 and ~2.6 times greater intensities of the peaks at 200 and 223 nm, respectively, in the CD spectrum of the mixed solution at equilibrium than in the CD spectrum of the acetic acid solution (Fig. 1). These results suggest that the 2+ and 3+ charge states correspond to PPII helix rich structures, whereas the 4+ charge state corresponds to more highly unfolded structures.

The acidified PTH_{64-84} solution was mixed with the aqueous ammonium acetate solution using theta-glass emitters with flow rates of ~48, ~120, and ~383 pL/s (Fig. 2c-e, respectively). These flow rates were obtained using various tip sizes and backing pressures[27] and correspond to reaction times of 1.0 ± 0.0, 3.0 ± 0.1, and 5.3 ± 0.2 μs, respectively.[27] These reaction times were obtained from the extent of folding that occurred during nanoESI for Trp-cage, a 20 residue mini-protein with a known folding time constant of 4.1 μs. The average charge of PTH_{64-84} decreases with increasing reaction time from 3.37 ± 0.03 at 1.0 μs to 2.78 ± 0.04 at 5.3 μs. At 5.3 μs (Fig. 2e), the average charge of PTH_{64-84} (2.78 ± 0.04) is the same within error as that obtained for the mixed solution at equilibrium (2.80 ± 0.01, Fig. 2b). At shorter reaction times (Fig. 2c and 2d), the average charge is higher than that obtained at equilibrium. These results indicate that the folding of PTH_{64-84} reaches equilibrium within 5.3 μs but not within 3.0 μs.

The folding time constant for the formation of the PPII helix conformation in PTH_{64-84} can be obtained from the extent of protein folding that occurs by modelling this reaction as a two state folding reaction.[33] Average charges can be used to determine the extent of folding and to obtain protein folding time constants [27] using the equation:

$$t = \tau \, ln \left(\frac{q_e - q_o}{q_e - q_t} \right) \quad (1)$$

where t is the reaction time, τ is the protein folding time constant, and q_e, q_o, and q_t are the average charges at equilibrium and at times 0 and t, respectively. The folding time constant

for the formation of the PPII helix structure in PTH_{64-84} is obtained from the rapid mixing data in which equilibrium is not reached (Fig. 2c and 2d) using eq 1. Folding time constants of 1.6 ± 0.2 and 1.4 ± 0.3 μs are obtained at reaction times of 1.0 and 3.0 μs, respectively (Fig. 2c and 2d). These values are the same within error, and the average value is 1.5 ± 0.3 μs. These results show that PTH_{64-84} folds from a highly unfolded structure to a mostly PPII helix structure within a few microseconds.

To confirm that PPII helices can form within this time frame, experiments were also performed with a second peptide with a PPII helix conformation. CD spectra of neurogranin fragment 28-43 (Ng_{28-43}) in a 100 mM aqueous acetic acid solution (pH = 2.9) and in the acetic acid solution mixed with a 100 mM aqueous ammonium acetate solution at a 1:1 ratio (equilibrium, pH = 4.7) are shown in Fig. 3 as dashed red and solid blue lines, respectively. There is only a small negative peak centered at 200 nm for the acetic acid solution. However, there are negative peaks at 202 and 233 nm and a positive peak at 219 nm for the premixed solution at equilibrium. A negative peak at 202 nm and a positive peak at 219 nm also occur in the CD spectrum of native polyproline, which adopts a PPII helix structure.[34] The similarities between the CD spectrum of native polyproline and that of Ng_{28-43} in the mixed solution at equilibrium indicates that Ng_{28-43} adopts a PPII helix conformation in the mixed solution. The weak negative peak centered at 233 nm may correspond to a small portion of Ng_{28-43} adopting an α-helix conformation. Two broad negative peaks centered at ~208 and ~222 nm are typically observed in the CD spectra of α-helices.[35] The negative peak normally observed at 208 nm may be unresolved from the strong negative peak at 202 nm. Overlap with the positive peak at 219 nm corresponding to α-helix regions of Ng_{28-43} may result in reduced signal intensity at 222 nm and thus an apparent shift to the higher 233 nm wavelength. The absence of peaks at 202, 219, and 233 nm in the CD spectrum of the acetic acid solution indicates that the majority of the PPII helix structure is disrupted in this solution.

Mass spectra of Ng_{28-43} in the acetic acid solution (pH = 2.9) and the acetic acid solution mixed with the ammonium acetate solution at a 1:1 ratio prior to nanoESI (equilibrium, pH = 4.7) are shown in Fig. 4a and 4b, respectively. With the acetic acid solution (Fig. 4a), the 3+ and 4+ charge states are formed and the 4+ is the most abundant (average charge = 3.95 ± 0.02). Ng_{28-43} is a 16 residue peptide, so 25% of the residues are charged in the 4+ charge state. To obtain similar extents of charging for ubiquitin and cytochrome c ions (27.6% and 23.1% of residues charged, respectively), the proteins must be significantly unfolded and the ions adopt near-linear conformations.[36] This result suggests that the 4+ charge state of Ng_{28-43} corresponds to highly unfolded conformations in solution. In the mass spectrum of the mixed solution at equilibrium (Fig. 4b), the 2–4+ charge states are formed and the 3+ is the most abundant (average charge = 3.04 ± 0.04). The average charge obtained from this solution is significantly less than that obtained with the acetic acid solution (3.95 ± 0.02). This result is consistent with Ng_{28-43} adopting a more folded structure in the mixed solution at equilibrium than in the acetic acid solution, consistent with the results obtained for these respective solutions using CD.

The acidified Ng_{28-43} solution was mixed with the ammonium acetate solution using the theta-glass emitters with a flow rate (~48 pL/s) that results in a reaction time of 1.0 μs (Fig.

4c). The 2–4+ charge states are formed with an average charge of 3.02 ± 0.04. This average charge is the same to within error as that obtained for a 1:1 mixture of these solutions at equilibrium (3.04 ± 0.04, Fig. 4b). This result indicates that the formation of the PPII helix structure in Ng_{28-43} reaches equilibrium within 1.0 μs. An upper limit to the folding time constant of Ng_{28-43} can be obtained with these results. An average charge of 3.10 (2σ above that obtained in the rapid mixing experiments) corresponds to a folding time constant of ~400 ns. To obtain the lower average charge of 3.02 obtained in the rapid mixing experiments would require an even shorter folding time constant. Therefore, the formation of the PPII helix in Ng_{28-43} occurs with a time constant of <400 ns. An approximate "speed limit" of n/100 μs, where n is the number of residues, has been reported for the folding of single-domain proteins and peptides.[1] Ng_{28-43} is a 16 residue peptide and thus has an approximate speed limit for folding of the entire peptide of 160 ns. The <400 ns folding time constant obtained for the formation of the PPII helix in Ng_{28-43} indicates that the PPII helix in this peptide must form at a rate very close to the speed limit for the formation of α-helix and β-structures in similarly sized peptides. In contrast, the 1.5 μs folding time constant for the formation of the PPII helix structure in PTH_{64-84} is about an order of magnitude greater than the approximate speed limit (210 ns for a 21 residue peptide). The significant difference in folding time constants obtained for these two peptides shows that the formation time of PPII helices from highly unfolded structures depends on the amino-acid sequence, consistent with results reported for the transition from PPI to PPII helices.[20-22]

Chemical processes that occur in these aqueous ESI nanodrops can potentially be affected by solvent evaporation, whi ch rapidly increases concentrations of less volatile components, and by interactions between molecules and the interface of the droplet surface. Bimolecular reactions can occur up to 10,000 times faster owing to these factors.[37,38] The unimolecular process of folding measured here should not be affected by concentration changes due to solvent evaporation at the low concentrations used (Supplementary Information), but interactions with the surface of the nanodrops may have an effect on folding rates compared to those in bulk solution.

Results from this study demonstrate that the formation of PPII helix structures can occur within a few microseconds or less in buffered aqueous solutions and that the formation of these structures can be monitored with mass spectrometry using rapid mixing from theta-glass emitters. To the best of our knowledge, the time constants measured here for the formation of PPII helix structures in buffered aqueous solutions are the first of their kind. These measurements should serve as useful benchmarks for comparisons with computational simulations. The formation time constants of other structures that fold on a similar time scale should be readily measurable using this technique.

Supplementary Material

Refer to Web version on PubMed Central for supplementary material.

Acknowledgments

Notes and references

1. Kubelka J, Hofrichter J, Eaton WA. Curr. Opin. Struct. Biol. 2004; 14:76–88. [PubMed: 15102453]

2. Lindorff-Larsen K, Piana S, Dror RO, Shaw DE. Science. 2011; 334:517–520. [PubMed: 22034434]

3. Lane TJ, Shukla D, Beauchamp KA, Pande VS. Curr. Opin. Struct. Biol. 2013; 23:58–65. [PubMed: 23237705]

4. Schweitzer-Stenner R. Mol. BioSyst. 2012; 8:122–133. [PubMed: 21879108]

5. Adzhubei AA, Sternberg MJE, Makarov AA. J. Mol. Biol. 2013; 425:2100–2132. [PubMed: 23507311]

6. Shoulders MD, Raines RT. Annu. Rev. Biochem. 2009; 78:929–958. [PubMed: 19344236]

7. Adzhubei AA, Sternberg MJE. J. Mol. Biol. 1993; 229:472–493. [PubMed: 8429558]

8. Bochicchio B, Tamburro AM. Chirality. 2002; 14:782–792. [PubMed: 12395395]

9. Cubellis MV, Caillez F, Blundell TL, Lovell SC. Proteins Struct. Funct. Bioinf. 2005; 58:880–892.

10. Berisio R, Loguercio S, De Simone A, Zagari A, Vitagliano L. Protein Peptide Lett. 2006; 13:847–854.

11. Shi ZS, Woody RW, Kallenbach NR. Adv. Protein Chem. 2002; 62:163–240. [PubMed: 12418104]

12. Zhu F, Kapitan J, Tranter GE, Pudney PDA, Isaacs NW, Hecht L, Barron LD. Proteins Struct. Funct. Bioinf. 2008; 70:823–833.

13. Shi ZS, Olson CA, Rose GD, Baldwin RL, Kallenbach NR. Proc. Natl. Acad. Sci. 2002; 99:9190–9195. [PubMed: 12091708]

14. Schweitzer-Stenner R, Measey TJ. Proc. Natl. Acad. Sci. 2007; 104:6649–6654. [PubMed: 17416675]

15. Detlefsen DJ, Thanabal V, Pecoraro VL, Wagner G. Biochemistry. 1991; 30:9040–9046. [PubMed: 1654086]

16. Elangovan S, Margolis HC, Oppenheim FG, Beniash E. Langmuir. 2007; 23:11200–11205. [PubMed: 17880251]

17. Pascal C, Pate F, Cheynier V, Delsuc M. Biopolymers. 2009; 91:745–756. [PubMed: 19402144]

18. Blanch EW, Morozova-Roche LA, Cochran DAE, Doig AJ, Hecht L, Barron LD. J. Mol. Biol. 2000; 301:553–563. [PubMed: 10926527]

19. Syme CD, Blanch EW, Holt C, Jakes R, Goedert M, Hecht L, Barron LD. Eur. J. Biochem. 2002; 269:148–156. [PubMed: 11784308]

20. Shi L, Holliday AE, Khanal N, Russell DH, Clemmer DE. J. Am. Chem. Soc. 2015; 137:8680–8683. [PubMed: 26115587]

21. Lin Y, Chu L, Horng J. J. Phys. Chem. B. 2015; 119:15796–15806. [PubMed: 26641495]

22. Shi L, Holliday AE, Glover MS, Ewing MA, Russell DH, Clemmer DE. J. Am. Soc. Mass Spectrom. 2016; 27:22–30. [PubMed: 26362047]

23. Mark LP, Gill MC, Mahutc M, Derrick PJ. Eur. J. Mass Spectrom. 2012; 18:439–446.

24. Fisher CM, Kharlamova A, McLuckey SA. Anal. Chem. 2014; 86:4581–4588. [PubMed: 24702054]

25. Mortensen DN, Williams ER. Anal. Chem. 2014; 86:9315–9321. [PubMed: 25160559]

26. Mortensen DN, Williams ER. Anal. Chem. 2015; 87:1281–1287. [PubMed: 25525976]

27. Mortensen DN, Williams ER. J. Am. Chem. Soc. 2016; 138:3453–3460. [PubMed: 26902747]

28. Jurchen JC, Williams ER. J. Am. Chem. Soc. 2003; 125:2817–2826. [PubMed: 12603172]

29. Weast, RC., editor. CRC Handbook of Chemistry and Physics. 55th ed.. CRC Press; Boca Raton, FL: 1974.

30. Fiskin AM, Cohn DV, Peterson GS. J. Biol. Chem. 1977; 252:8261–8268. [PubMed: 562343]

31. Kaltashov I, Eyles S. Mass Spectrom. Rev. 2002; 21:37–71. [PubMed: 12210613]

32. Liu J, Konermann L. J. Am. Soc. Mass Spectrom. 2009; 20:819–828. [PubMed: 19200750]

33. Gilmanshin R, Callender R, Dyer R. Nat. Struct. Biol. 1998; 5:363–365. [PubMed: 9586997]

34. Lopes JLS, Miles AJ, Whitmore L, Wallace BA. Protein Sci. 2014; 23:1765–1772. [PubMed: 25262612]

35. Greenfield NJ, Fasman GD. Biochemistry. 1969; 8:4108–4116. [PubMed: 5346390]

36. Going CC, Williams ER. Anal. Chem. 2015; 87:3973–3980. [PubMed: 25719488]

37. Badu-Tawiah AK, Campbell DI, Cooks RG. J. Am. Soc. Mass Spectrom. 2012; 23:1461–1468. [PubMed: 22825741]

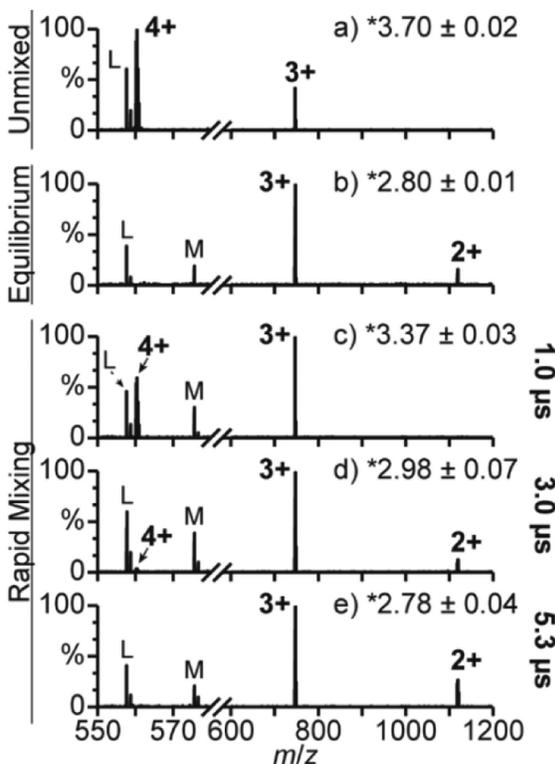38. Bain RM, Pulliam CJ, Ayrton ST, Bain K, Cooks RG. Rapid Commun. Mass Spectrom. DOI: 10.1002/rcm.7664.
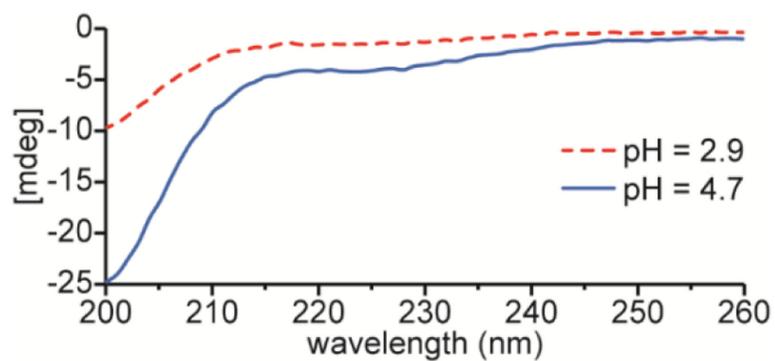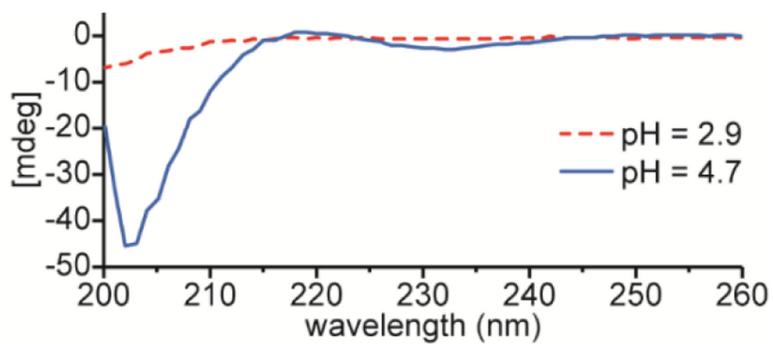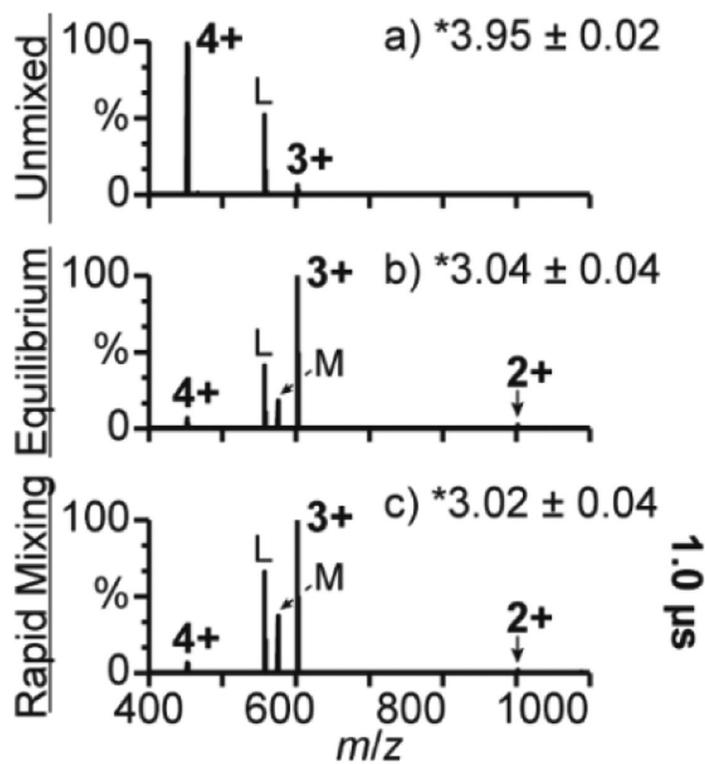
Fig. 1.
Circular dichroism spectra of PTH$_{64-84}$ in a 100 mM aqueous acetic acid solution (pH = 2.9, dashed red line) and the acetic acid solution mixed with a 100 mM aqueous ammonium acetate solution at a 1:1 ratio (equilibrium, pH = 4.7, solid blue line).

Fig. 2.
Mass spectra of (a) PTH$_{64-84}$ in a 100 mM aqueous acetic acid solution (pH = 2.9), (b) the acetic acid solution mixed with a 100 mM aqueous ammonium acetate solution at a 1:1 ratio prior to nanoESI (equilibrium, pH = 4.7), and (c) the acetic acid solution mixed with the ammonium acetate solution using the theta-glass emitters with flow rates that result in reaction times of (c) 1.0, (d) 3.0, and (e) 5.3 μs. (*) denotes average charge state. (L) and (M) denote Leu- and Met-enkephalin, respectively, which are used as internal standards to measure the relative flow rates of the solutions in the individual barrels of the theta-glass emitters.

Fig. 3.
Circular dichroism spectra of Ng$_{28\text{-}43}$ in a 100 mM aqueous acetic acid solution (pH = 2.9, dashed red line) and the acetic acid solution mixed with a 100 mM aqueous ammonium acetate solution at a 1:1 ratio (equilibrium, pH = 4.7, solid blue line).

Fig. 4.
Mass spectra of (a) Ng$_{28-43}$ in a 100 mM aqueous acetic acid solution (pH = 2.9), (b) the acetic acid solution mixed with a 100 mM aqueous ammonium acetate solution at a 1:1 ratio prior to nanoESI (equilibrium, pH = 4.7), and (c) the acetic acid solution mixed with the ammonium acetate solution using the theta-glass emitters with a flow rate that results in a reaction time of 1.0 μs. (*) denotes average charge state. (L) and (M) denote Leu- and Met-enkephalin, respectively, which are used as internal standards to measure the relative solution flow rates.